# UC Irvine

**Title**

Retinal transplants restore visual responses: trans-synaptic tracing from visually responsive sites labels transplant neurons

**Permalink**

https://escholarship.org/uc/item/7d9054n7

**Journal**

European Journal of Neuroscience, 28(1)

**ISSN**

0953-816X

**Authors**

Seiler, Magdalene J
Thomas, Biju B
Chen, Zhenhai
et al.

**Publication Date**

2008-07-01

**DOI**

10.1111/j.1460-9568.2008.06279.x

Peer reviewed

# Retinal transplants restore visual responses: trans-synaptic tracing from visually responsive sites labels transplant neurons

Magdalene J. Seiler,[1,2,]* Biju B. Thomas,[1] Zhenhai Chen,[1] Rongjuan Wu,[1] Srinivas R. Sadda[1] and Robert B. Aramant[3,]*

[1]Ophthalmology-USC, Doheny Eye Institute, 1355 San Pablo Street, DVRC 402, Los Angeles, CA 90033, USA
[2]Cell & Neurobiology-USC, Los Angeles, CA, USA
[3]Anatomical Sciences & Neurobiology, University of Louisville, Louisville, KY, USA

## Abstract

This study aimed to test the hypothesis that visual responses in the superior colliculus (SC) originate from synaptic connections between fetal retinal transplants and degenerating host retinas. Sheets of embryonic day 19 rat retina expressing human placental alkaline phosphatase were transplanted to the subretinal space of 3- to 4-week-old S334ter-line-3 rats with fast retinal degeneration. Several months later, visual responses were recorded from the SC. Attenuated pseudorabies virus that is specifically transferred between neurons at synapses (strains PRV-152, expressing green fluorescent protein (GFP) or BaBlu, expressing *Escherichia coli* β-galactosidase) was injected into the visually responsive site of the SC. After survival times of 1–2 days, the virus was detected in the retina by immunohistochemistry in combination with different retinal cell markers, such as protein kinase C, recoverin, calcium-calmodulin-dependent protein kinase II and glutamine synthetase. Transplanted rats had a mean response threshold of −3.1 log cd/m² in a small area of the SC corresponding to the location of the graft in the retina. By 30 h after injection into this SC area, the virus traced back to host ganglion cells overlying the transplant and in close proximity to the transplant. By 2 days after injection, extensive virus label was found in the host retina and many cells in the transplant were also labeled. Virus-labeled cells in the transplant were double labeled for neuronal and glial cell markers. This study provides anatomical evidence that synaptic connections between fetal retinal transplants and host retinas contribute to the visual responses in the SC.

## Introduction

Incurable diseases affecting photoreceptors and the retinal pigment epithelium may leave the inner retina functional for some time (Milam *et al.*, 1998; Humayun *et al.*, 1999). If cells could replace the degenerating photoreceptors and connect to the remaining inner retina it may be possible to restore vision.

Numerous groups have transplanted retinal progenitor cells as dissociated cells (Kwan *et al.*, 1999; Klassen *et al.*, 2004; MacLaren *et al.*, 2006), microaggregates (Gouras & Tanabe, 2003) or retinal sheets (Ghosh *et al.*, 2004; Aramant *et al.*, 2006) to various models of retinal degeneration.

Retinal progenitor sheets transplanted to the subretinal space of retinal-degenerate recipients (for review see Aramant & Seiler, 2004; Seiler & Aramant, 2005) develop photoreceptors with inner and outer segments in contact with the host or donor retinal pigment epithelium (Seiler & Aramant, 1998; Aramant *et al.*, 1999). Transplant photo-receptors show a shift in the distribution of phototransduction proteins in response to light like normal photoreceptors (Seiler *et al.*, 1999). Allogeneic transplants also appear to be tolerated in the subretinal space, without need for immunosuppression (Aramant & Seiler, 2002).

Retinal transplants to rodent retinal degeneration models can restore visual responses in the superior colliculus (SC) within an area that topographically matches the transplant placement in the retina (Woch *et al.*, 2001; Sagdullaev *et al.*, 2003; Arai *et al.*, 2004; Thomas *et al.*, 2004), using the well-established topographic map of the retina on the SC surface (O'Leary *et al.*, 1986; Simon & O'Leary, 1992). Such responses can be recorded at lower light levels and with shorter response onset latencies than at the time of transplantation (Thomas *et al.*, 2006). The neuronal processes of transplant cells can cross between the transplant and host retina (Aramant & Seiler, 1995; Ghosh *et al.*, 1999; Gouras & Tanabe, 2003).

Attenuated pseudorabies virus (PRV) (PRV Bartha and derived recombinant strains, such as PRV-Bablu or PRV-152) is an established tool for outlining multisynaptic circuitry in the central nervous system (Card *et al.*, 1990). These viruses are specifically transferred between neurons at synapses and are only transported in a retrograde direction (Card *et al.*, 1993). Virus transfer depends on the development of functional synapses (Rinaman *et al.*, 2000). Only neurons, not glial cells, can assemble the virus envelope necessary for transfer of the virus to another cell (Card *et al.*, 1993). PRV has a high affinity for nerve terminals (Marchand & Schwab, 1986) and astrocytic membranes. Astrocytes enclosing a synapse with their processes will also be infected but cannot assemble the virus envelope and consequently will not release infectious virus, thus preventing non-specific virus spread (Card *et al.*, 1993; Card, 1998). After injection of PRV into the SC in an area corresponding to the placement of the transplant in the retina, neuronal

*Correspondence*: Dr. Biju B. Thomas, as above.
E-mail: bthomas@doheny.org

*Present address*: Anatomy & Neurobiology, Reeve-Irvine Research Center, UC Irvine, CA, USA.

TABLE 1. Overview of experiments

| Rat no. | Age at recording (weeks) | Response quality | Visual threshold (log cd/m$^2$) | Virus strain PRV | Survival after injection (h) | Host label (labeled host GC/section analyzed) | % Host label over graft* | Graft label[†] | Transplant morphology |
|---|---|---|---|---|---|---|---|---|---|
| 1 | 12.4 | Good | −1.7 | 152 | 30.0 | 0.5 (graft edge) | 55.6 | 0 | Rosettes |
| 2 | 12.3 | Weak | −2.9 | Bablu | 34.0 | 18.6 (over graft) | 68.6 | 0.4 | Rosettes |
| 3 | 22.9 | Weak | −1.1 | Bablu | 50.2 | 0.5 (over graft) | 42.1 | 0.1 | Rosettes |
| 4 | 14 | Good | −2.3 | Bablu | 47.5 | 7.0 (graft edge) | 53.6 | 0.6 | Small laminated area + rosettes |
| 5 | 13.9 | Weak | −1.7 | Bablu | 47.0 | 4.3 (over graft) | 91.1 | 0.7 | Rosettes |
| 6 | 16.4 | Weak | −2.9 | 152 | 46.3 | 8.6 (graft edge) | 66.1 | 1.5 | Large laminated area, part separated; + rosettes |
| 7 | 22.9 | Good | −3.5 | Bablu | 48.0 | 8.7 (over graft) | 79.8 | 1.7 | Rosettes |
| 8 | 12.4 | Weak | −2.9 | Bablu | 47.6 | 24.55 (over part) of graft) | 57.4 | 3.2 | Small laminated area + mostly rosettes; small part epiretinal |
| 9 | 13.9 | Weak | −2.9 | Bablu | 48.6 | 42.25 (over graft) | 89.25 | 7.7 | Small laminated area + mostly rosettes; part separated |
| 10 | 16.3 | Good | −3.5 | Bablu | 52.1 | 13 (over and adjacent to graft) | 96.0 | 8.1 | Several laminated areas + rosettes; laminated area bridging host retina |
| 11 | 23.9 | Good | −3.5 | Bablu | 51.7 | 37.8 (over and adjacent to graft) | 70.5 | 11.2 | Rosettes |
| 12 | 13.1 | Weak | −3.5 | 152 | 46.3 | 60.5 (over and adjacent to graft) | 56.6 | 25.5 | Laminated area + rosettes, part of graft epiretinal |
| 13 | 14.3 | Weak | −2.9 | 152 | 52.8 | 132.1 (over and adjacent to graft) | 49.4 | 32 | Rosettes |
| 14 | 17.7 | Weak | −2.9 | 152 | 53.5 | 140.5 (over and adjacent to graft) | 38.3 | 55.3 | Laminated area + rosettes |

PRV, pseudorabies virus. *PRV-labeled cells in host ganglion cell layer (GCL) over graft/total number of PRV-labeled cells in GCL. [†]Average no. of labeled cells in graft/per graft section.

cells are labeled in retinal progenitor sheet transplants (Seiler *et al.*, 2005).

Recently, another group combined visual electrophysiology with PRV trans-synaptic tracing in the visual system to identify local retinal circuits of melanopsin-containing retinal ganglion cells (Viney *et al.*, 2007). Trans-synaptic labeling of transplanted neurons, however, has never been correlated with visual electrophysiologic responses.

The goal of this study was to demonstrate that synaptic connections are involved in visual responses in retinal-degenerate rats with retinal sheet transplants. This was accomplished by trans-synaptic tracing specifically from the visually responsive site in the SC back to the retina, using the attenuated PRV strains PRV-BaBlu and PRV-152 expressing GFP.

## Materials and methods

### Animals

For all experimental procedures, animals were treated in accordance with the NIH guidelines for the care and use of laboratory animals and the ARVO Statement for the Use of Animals in Ophthalmic and Vision Research, and under a protocol approved by the Institutional Animal Care and Use Committee of the Doheny Eye Institute, University of Southern California. All efforts were made to use only the minimum number of animals necessary to provide an adequate sample size. Sixty transgenic pigmented S334ter-line-3 retinal-degenerate rats expressing a mutated human rhodopsin protein (Sagdullaev *et al.*, 2003) received retinal sheet transplants in one eye at postnatal days 24–35. Of these, 23 animals (38%) were selected for this virus tracing study based on responses in the SC (see below). Nine rats died prematurely after the virus injection, so 14 rats (23%) were left for the analysis described in this study.

Most of the procedures used in these experiments have been described in detail elsewhere (Woch *et al.*, 2001; Sagdullaev *et al.*, 2003; Thomas *et al.*, 2004; Seiler *et al.*, 2005) and will be briefly described.

### Donor tissue

Transgenic rats carrying the human placental alkaline phosphatase (hPAP) gene (Kisseberth *et al.*, 1999) were used as the source of donor tissue for these studies. For some experiments, rats expressing both GFP and hPAP were used as donors. These were derived from a cross between hPAP and GFP transgenic rats (Hakamata *et al.*, 2001). Rats were mated and mating was confirmed by vaginal smears. Timed-pregnant rats were anesthetized by intraperitoneal injection of ketamine (37.5–50 mg/kg) and xylazine (5–10 mg/kg) and killed after the C-section with an overdose of sodium pentoborbital (240 mg/kg). Fetuses were removed by Caesarean section at days 18–20 of gestation (day of conception = day 0). Most of the rats received embryonic day 19 donor tissue, with the exception of one rat that received embryonic day 18 and two rats that received embryonic day 20 transplants. A small piece of the fetus's tail or limbs was tested by histochemistry for hPAP (Kisseberth *et al.*, 1999) to identify transgenic fetuses. Embryos were stored in Hibernate E medium (Brainbits, Springfield, IL, USA) with B-27 supplements (InVitrogen, Carlsbad, CA, USA) for up to 6 h. The retinal tissue was flattened in a drop of medium. Retinal progenitor sheets were cut into rectangular pieces of 1–1.5 × 0.6 mm to fit into the previously described custom-made implantation tool (Seiler & Aramant, 1998; Aramant & Seiler, 2002). Immediately before implantation, the tissue was taken up in the correct orientation (ganglion cell side up) into the flat nozzle of the implantation tool.

In eight of 14 experiments, fetal sheets were embedded in a neurite outgrowth-promoting matrix (thiolated hyaluronic acid matrix) (Shu *et al.*, 2002). In six experiments, retinal sheets were incubated in brain-derived neurotrophic factor (BDNF) microspheres (Mahoney & Saltzman, 2001). In four experiments, both procedures were combined. The experiments described in this study extended over several years and thus some experimental transplant procedures were changed over time.

### Transplantation

Rats were anesthetized by intraperitonieal injection with ketamine (37.5 mg/kg) and xylazine (5 mg/kg). The superior area of the left eye

TABLE 2. Antibodies used

| Antibodies | Species | Specific for | Dilution | Supplier |
|---|---|---|---|---|
| Primary antibodies | | | | |
| PRV | Rabbit | PRV | 1 : 5000 | Enquist (Card *et al.*, 1990), Princeton University, NJ, USA |
| | | | 1 : 20 000 with ABC method | |
| hPAP | Mouse | hPAP | 1 : 100 | Cymbus Biotechnology, Eastleigh, UK |
| | | | 1 : 600 | Sigma, St Louis, MO, USA |
| Glutamine synthetase | Mouse | Glial cells | 1 : 1000 | Transduction Labs, Lexington, KY, USA |
| Protein kinase C | Mouse | Rod bipolar cells | 1 : 100 | Biodesign, Saco, ME, USA |
| Recoverin | Mouse | Cone bipolar cells; photoreceptors (rods + cones) | 1 : 500 | McGinnis *et al.* (1997), University of Oklahoma, OK, USA |
| Parvalbumin | Mouse | Amacrine cells + horizontal cells | 1 : 500 | Sigma, St Louis, MO, USA |
| NeuN | Mouse | Neurons | 1 : 200 | Chemicon, Temecula, CA, USA |
| CaMKII | Mouse | Calcium-calmodulin-dependent kinase II (neurons) | 1 : 100 | Chemicon, Temecula, CA, USA |
| MAP-2 | Mouse | Neuronal cell processes | 1 : 500 | Chemicon, Temecula, CA, USA |
| MAP-1A | Mouse | Neuronal cell processes, ganglion cell dendrites | 1 : 1000 | Amersham, Pittsburgh, PA, USA |
| Calbindin | Mouse | Horizontal + amacrine cells, cones | 1 : 2000 | Calbiochem, San Diego, CA, USA |
| Secondary antibodies | | | | |
| Rhodamine RedX α-mouse IgG | Goat | Mouse antibodies | 1 : 200 | Molecular Probes, Eugene, OR, USA |
| AF 488 α-rabbit IgG | Goat | Rabbit antibodies | 1 : 200 | Molecular Probes, Eugene, OR, USA |
| Biotin anti-rabbit IgG | Horse | Rabbit antibodies | 1 : 200 | Vector Laboratories, Burlingame, CA, USA |
| Elite ABC | n.a. | Biotin | 1 : 200 | Vector Laboratories, Burlingame, CA, USA |

PRV, pseudorabies virus; CaMKII, calcium-calmodulin-dependent protein kinase II; IgG, immunoglobulin G; MAP, microtubule-associated protein; n.a., not applicable.

between two varicose veins was exposed. A transverse incision (< 1 mm) was cut through the sclera, choroid and retina using a microknife (World Precision Instruments, Sarasota, FL, USA). The loaded implantation instrument was inserted into the subretinal space and advanced further centrally, nasal to the optic disc. When the target area was reached, the tissue was placed into the subretinal space and the instrument withdrawn. Care was taken not to injure the host retinal pigment epithelium. The incision site was closed with 10-0 sutures and the cornea covered with artificial tears ointment. Rats recovered from anesthesia in a Thermocare incubator.

### SC recording

At 9–19 weeks after transplantation (age 12–24 weeks), electrophysiological assessment of visual responses in the SC was performed as previously described (Thomas *et al.*, 2005). Seven rats were analyzed at 12–14 weeks of age, four rats at 16–18 weeks of age, and three rats at 22–24 weeks of age (see Table 1). Briefly, the rats were dark-adapted overnight (< −6.00 log cd/m$^2$). The eyes were covered with a custom-made eye-cap to prevent bleaching of the photoreceptors during surgery. After initial intraperitoneal injection of ketamine/xylazine (37.5 mg/kg ketamine and 5 mg/kg xylazine), a gas inhalant anesthetic (1.0–2.0% halothane in 40% O$_2$/60% N$_2$O) was administered via an anesthetic mask (Stoelting Company, Wood Dale, IL, USA). Multi-unit visual responses were recorded extracellularly from the superficial laminae of the exposed SC using nail-polish-coated tungsten microelectrodes. A full-field light stimulus (controlled by a camera shutter) was projected on the back of a white plexiglass screen (diameter 20 cm) placed 10 cm in front of the contralateral eye (duration 50 ms) for the recordings. A significant visual response was defined as the point at which a clear, prolonged (> 20 ms) activity

TABLE 3. Double-stained cells in graft (selected antibodies)

| Antibody | Confocal images (*n*) | Sections analyzed (*n*) | PRV-positive transplant cells that are double stained for antigen (%) |
|---|---|---|---|
| Glutamine synthetase | 25 | 8 | 13.25 ± 5.5 (0–27.3) |
| PKC | 15 | 5 | 8.4 ± 3.0 (2.2–15.8) |
| CaMKII | 22 | 6 | 13.1 ± 5.0 (0–20.7) |
| Recoverin | 18 | 6 | 3.3 ± 1.9 (2.2–3.9) |
| MAP-2 | 14 | 5 | 23.5 ± 7.2 (0–100) |
| Parvalbumin | 17 | 4 | 0.9 ± 0.6 (0–9.1) |
| NeuN | 9 | 4 | 25.1 ± 6.08 (0–57.1) |

Data were presented as mean ± SEM (and range). Percentage of virus-labeled cells in transplant that were double stained for the glial marker glutamine synthetase, or the neural markers protein kinase C (PKC), calcium-calmodulin-dependent protein kinase II (CaMKII) or recoverin (data from three to four experiments). MAP, microtubule-associated protein.

increase (at least twice) could be measured above the average background activity, which was determined using the 100 ms of recording preceding the light flash. Spontaneous activity was apparent with a higher light intensity stimulus; however, the visual responses could be easily distinguished because of their consistency in amplitude and latency.

The intensity of the light stimulus at the beginning of the recording was set at −6.46 log cd/m$^2$ and gradually increased (by steps of 0.25 log cd/m$^2$ controlled by neutral density filters) up to 0.81 log cd/m$^2$. Starting with the lowest light levels, the superficial layer of the SC was mapped systematically with ca. 200 μm between penetration sites. At each stimulus intensity step, the visual stimulus was presented

**Low Threshold** | **High Threshold**

good
responses

weak
responses

- 3.5    - 2.3    - 1.1

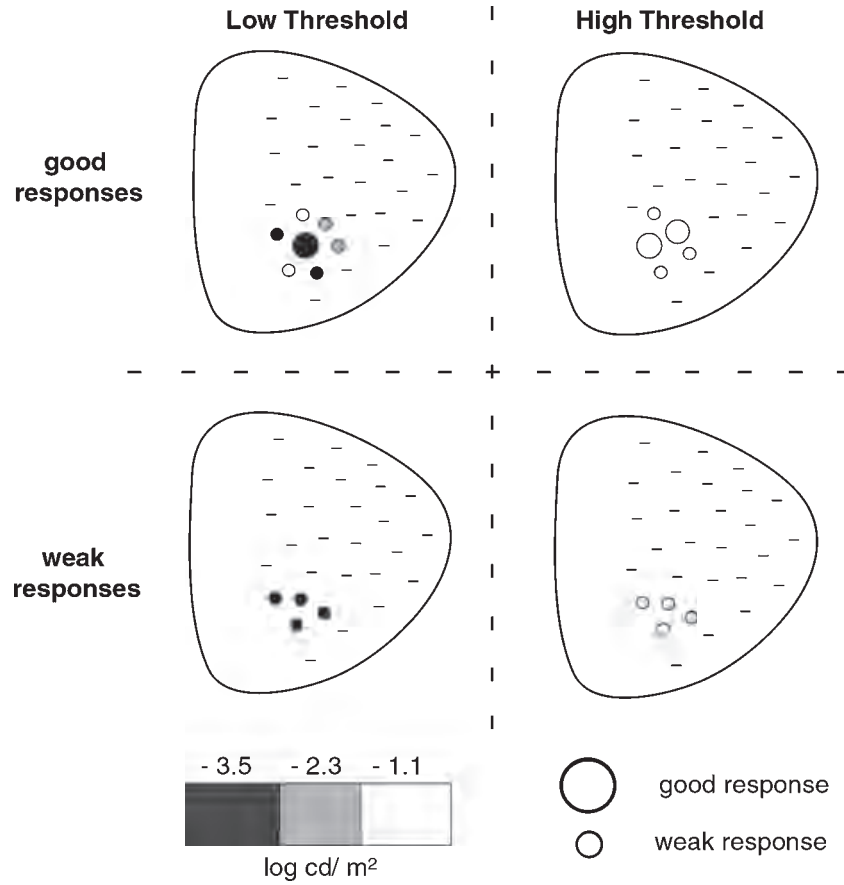log cd/ m²

good response

weak response

FIG. 1. Response characteristics in the SC from transplanted retinal-degenerate rats (schematic diagram). Response thresholds were determined by testing at different light intensities from an area corresponding to the transplant location in the eye (see Table 1). The light intensities are indicated by black, gray, and white. The two different response types are: (i) robust spike activity (good responses; large circles) and (ii) weak spike activity (weak responses; small circles) (see traces in Fig. 2 for examples). Dashes indicate absence of responses.

**Good response**          **Weak response**

dim
light

- 3.1
log cd/m²

strong
light

- 1.1
log cd/m²

Light          20 mV
Stimulus

100 ms
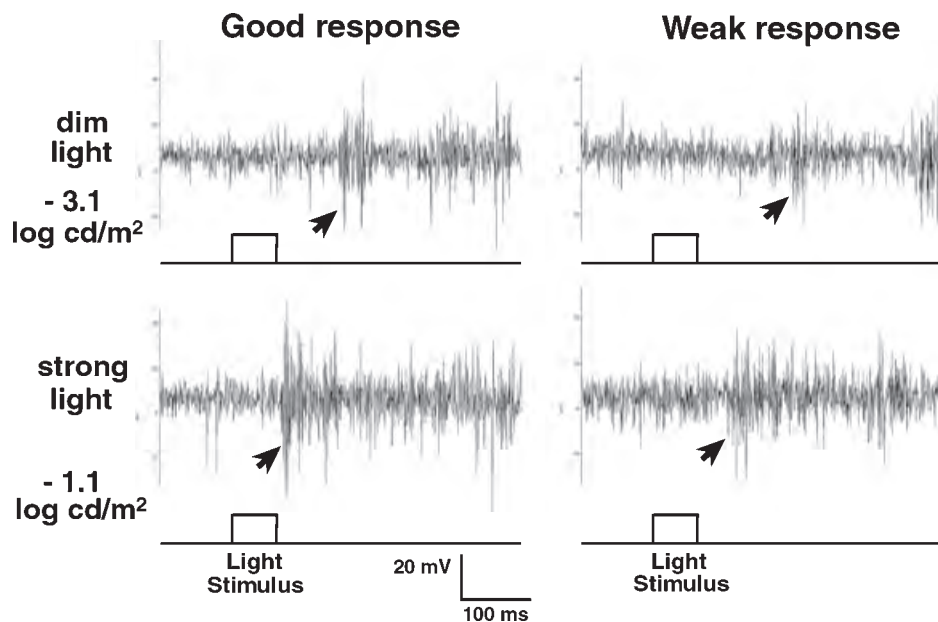
Light
Stimulus

FIG. 2. Examples of traces from rats no. 10 (left column) and no. 12 (right column) at two different light intensities (−3.1 cd/m² and −1.1 log cd/m²). The duration of the light stimulus was 60 ms. The onset of the visual response is indicated by arrows. 'Good-response' recordings are characterized by robust spike activity in response to increase in stimulus strength, whereas such an increase in spike activity is less apparent for 'weak responses'.
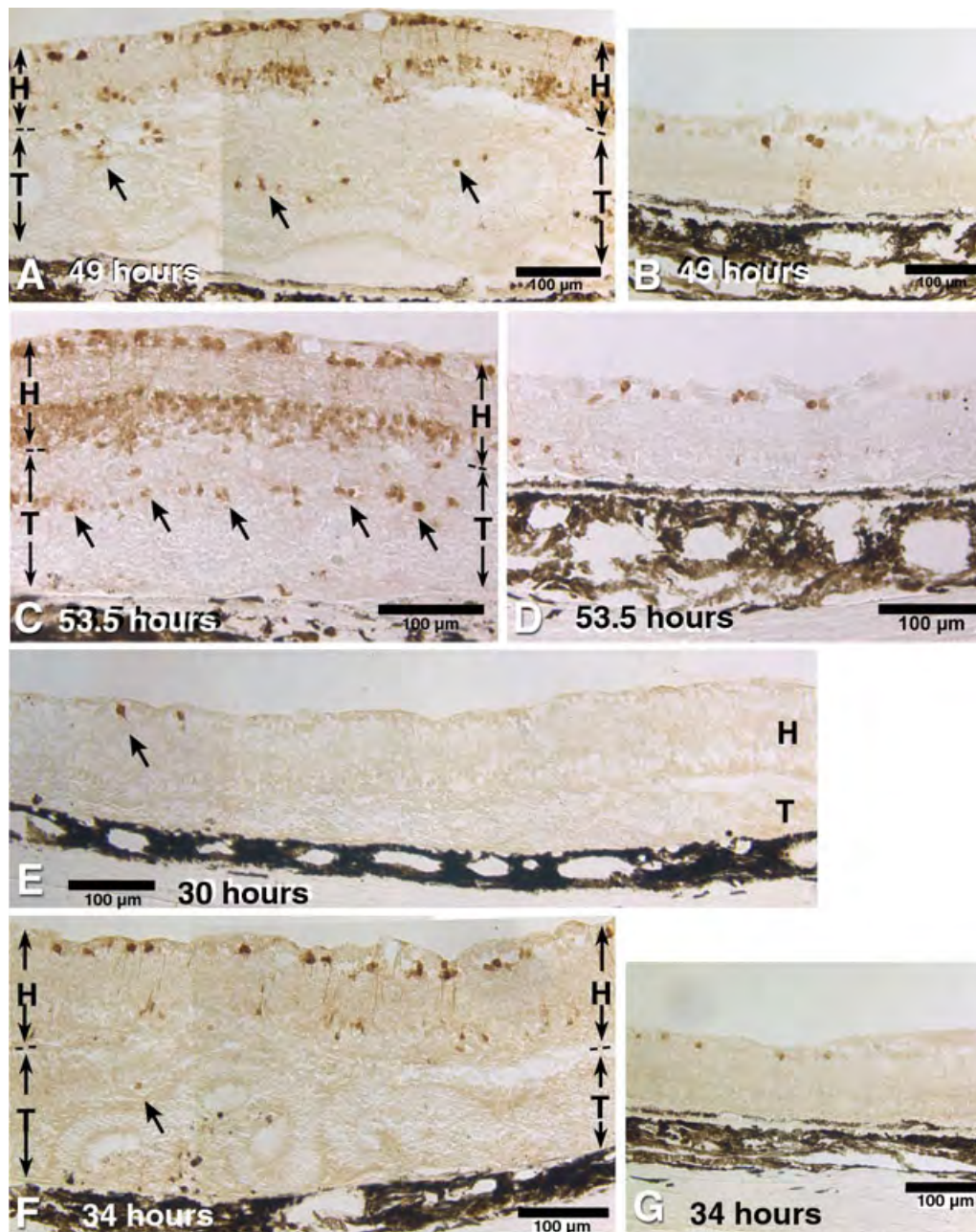
FIG. 3. Pseudorabies virus label after different survival times (see also Table 1). (A and B) Rat no. 9 at 49 h after virus. (A) Arrows point to PRV-labeled cells in transplant. (B) Secondary label in adjacent host retina. (C and D) Rat no. 14 at 53.5 h after virus. (C) Strong label of transplant cells (arrows). (D) Some lateral secondary label in adjacent host retina (mainly ganglion cells). (E) Rat no. 1 at 30 h after virus. Few host ganglion cell layer labeled (arrow) and no label in graft. (F and G) Rat no. 2 at 34 h after virus. (F) Strong label in host retina over transplant, one PRV-labeled cell in graft (arrow). (G) Some labeled ganglion cells in adjacent host retina but less label, indicating that the virus was transferred there secondarily. H, host; T, transplant. Bars, 100 μm.

at least six times with an interval of 10 s between the stimuli. As a control, blank stimuli were given in which the light stimulus was blocked by an opaque filter. All electrical activity was recorded using a digital data-acquisition system (Powerlab; ADI Instruments, Mountain View, CA, USA).

### Statistical analysis

Statistical comparisons were made using the Fisher exact probability test and a one-way ANOVA with subsequent *post hoc* tests using a

statistics package of GraphPad Software, Inc. (San Diego, CA, USA).

### Virus strain used

Attenuated PRV of the Bablu strain (expressing *Escherichia coli* β-galactosidase) (Loewy *et al.*, 1991; Kim *et al.*, 1999) and of the PRV-152 strain (expressing green fluorescent protein) (Pickard *et al.*, 2002) was received from Dr. L.W. Enquist (Princeton University, NJ, USA). Both virus strains are derived from PRV Bartha and have similar properties
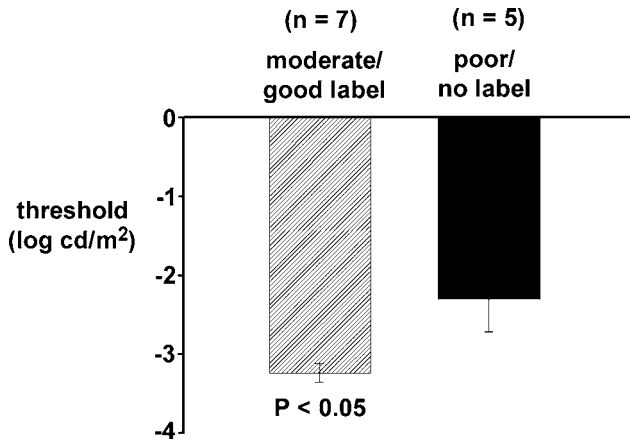
FIG. 4. Virus label in transplant vs. visual threshold. Comparison of PRV label in transplant with 2 days following virus injection (12 rats). Rats were divided into two groups: 'moderate/strong labeling' (3.2–55.3 cells in graft/graft section; 24.55–140.5 cells in host GCL/section) (rats 8–14; $n = 7$) and 'poor/no labeling' (0–1.7 cells in graft/graft section; 0.5–8.7 cells in host GCL/section) (rats 3–7; $n = 5$). Two-tailed $P < 0.05$ (unpaired Student's $t$-test), indicating a significant difference.

(Cano *et al.*, 2004). Originally, we used with PRV-152. However, for animals that received donor tissue expressing both hPAP and GFP, the BaBlu virus had to be used. The virus was shipped on dry ice, thawed on ice, immediately aliquoted and stored at $-80$ °C. Virus concentrations were in the range of $7$–$8 \times 10^{8}$ plaque-forming units/mL.

## Virus tracing

For the virus tracing experiments, 23 transplanted rats were selected that showed visual responses in a specific area of the SC (corresponding to 38% of all transplant experiments). Of these 23 rats, nine died before they could be perfused with fixative 2 days later; thus, 14 rats were left for analysis (see Table 1). The high death rate in the initial experiments was due to the long duration of recording of the exposed brain, which caused brain edema. This problem was later solved by treatment with dexamethasone and lactated glucose ringer.

As the virus injection was not allowed in the vivarium for biosafety reasons, anesthetized rats were moved after electrophysiological recording from the vivarium to a virus injection area beside a fume hood and placed again into a stereotactic frame under halothane anesthesia (same anesthesia as for SC recording). The best visually responsive site on the SC surface was identified based on superficial landmarks (blood vessels). A glass needle with a beveled tip (I.D. 70 μm) was filled with virus in a fume hood and attached to a filled 0.5 μL Hamilton syringe. Either PRV-Bablu or PRV-152 (100 nL) was injected at a rate of 10 nL/min (see Table 1) using an ultramicropump (World Precision Instruments) at a depth of 0.3 mm from the exposed SC surface. To prevent leakage of the virus solution, the needle was left in place for at least 5 min before it was withdrawn. After closing the hole with sterile gel foam, the wound was sutured, the rats recovered in an incubator and were allowed to survive for 2 days in a microisolator cage with access to food and water *ad libitum*. Rats were injected pre- and postoperatively with dexamethasone (5 mg/kg) to prevent brain edema. The rats were given i.v. infusions with lactated glucose ringer (Hospira Inc., Lake Forest, IL, USA) every 3–4 h on the first day following the injection to prevent dehydration. Twelve rats were perfused at

46–53 h after injection but two rats had to be perfused with fixative prematurely at 30–34 h because they would not have survived further (see Table 1).

## Tissue processing

Rats were injected intraperitoneally either with an overdose of Na-pentobarbital (240 mg/kg) or an overdose of ketamine/xylazine (100 mg/kg ket, 20 mg/kg xyl). Animals were perfused through the ascending aorta (with the descending aorta clamped off) with 120 mL 0.9% saline followed by 300 mL 4% paraformaldehyde/0.1% glutaraldehyde in 0.1 M sodium phosphate buffer, pH 7.2. Both eyes and the brain were removed and placed in fixative. After 10–20 min in fixative, the cornea was removed, tissues postfixed for another 60–90 min and then washed with 0.1 M sodium phosphate buffer. After dissection, eyecups were infiltrated with 30% sucrose overnight and frozen in Tissue Tek in methylbutane on dry ice. Serial sections were cut at 10 μm on a Leica cryostat.

## Immunohistochemistry

For an initial scanning of the experiments, every fifth slide was stained using a polyclonal rabbit antiserum against PRV (Card *et al.*, 1990; Card & Enquist, 1994), generously provided by L.W. Enquist (Princeton University) and J.P. Card (University of Pittsburgh), at a concentration of 1 : 20 000 overnight at 4 °C, followed by several washes with phosphate-buffered saline (0.1 M NaCl, 0.05 M sodium phosphate buffer, pH 7.2), biotinylated anti-rabbit immunoglobulin G (raised in goat) and the Elite-ABC kit with horseradish peroxidase (Vector Laboratories, Burlingame, CA, USA). A diaminobenzidine kit (Vector Laboratories) was used as substrate.

All PRV-labeled cells in the host ganglion cell layer (overlying and outside the transplant area) and transplant were counted on these sections. The number of cells in the host ganglion cell layer and graft was then divided by the number of analyzed sections to obtain the average number of labeled cells/section. The percentage of labeled cells in the host ganglion cell layer overlying the graft was also calculated (see Table 1).

In a subgroup of experiments (five rats; four with survival time of 46–53 h and one with survival time of 30 h), selected slides were double stained using a combination of the PRV antiserum at a dilution of 1 : 5000 together with various mouse monoclonal antibodies (see Table 2). Of the three sections on a slide, one section was stained with a combination of mouse anti-hPAP (donor cell label) and rabbit anti-PRV, and the two adjacent sections with other combinations of mouse antibodies with the rabbit anti-PRV antibody. The primary antibodies were detected by Alexa Fluor 488-conjugated anti-rabbit immunoglobulin G and Rhodamine RedX anti-mouse immunoglobulin G (Molecular Probes) at a dilution of 1 : 200 (see Table 2). Cell nuclei were stained with 4′6-diamidino-2-phenylindole dihydrochloride-containing mounting medium (Vector Laboratories). Fluorescent images (two to six microscopic fields per section) were scanned in an LSM510 confocal microscope (Carl Zeiss, Germany). Five to seven images of one field at several focus depths were combined into one image.

Confocal images of virus-labeled cells in the transplant were all taken at the same magnification of 40× (examples in Figs 4–8). For a semiquantitative analysis, the total number of virus-labeled cells and the number of double-stained cells was counted in the transplant only. The location of the transplant was determined by the hPAP staining on adjacent sections. The 'number of sections' in Table 3 refers to the total number of sections analyzed.
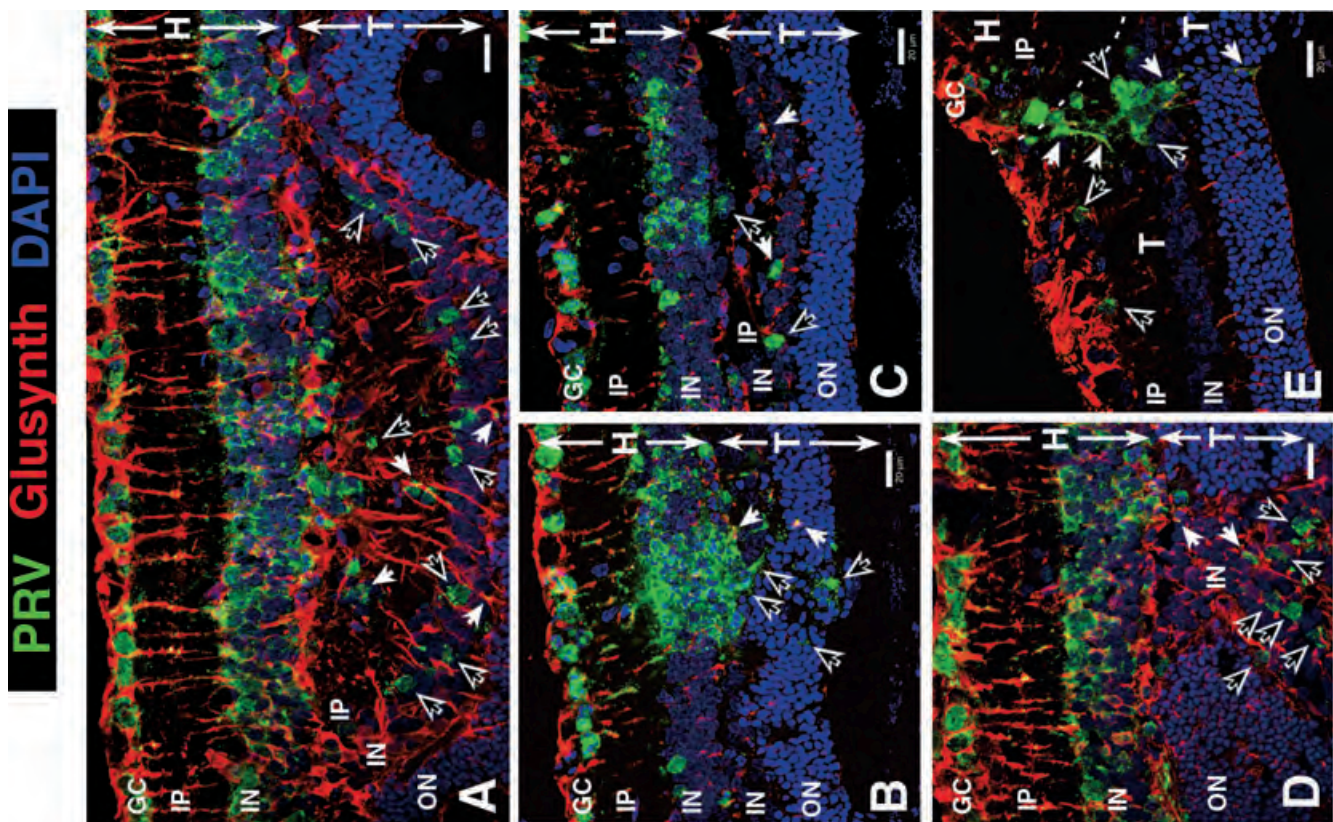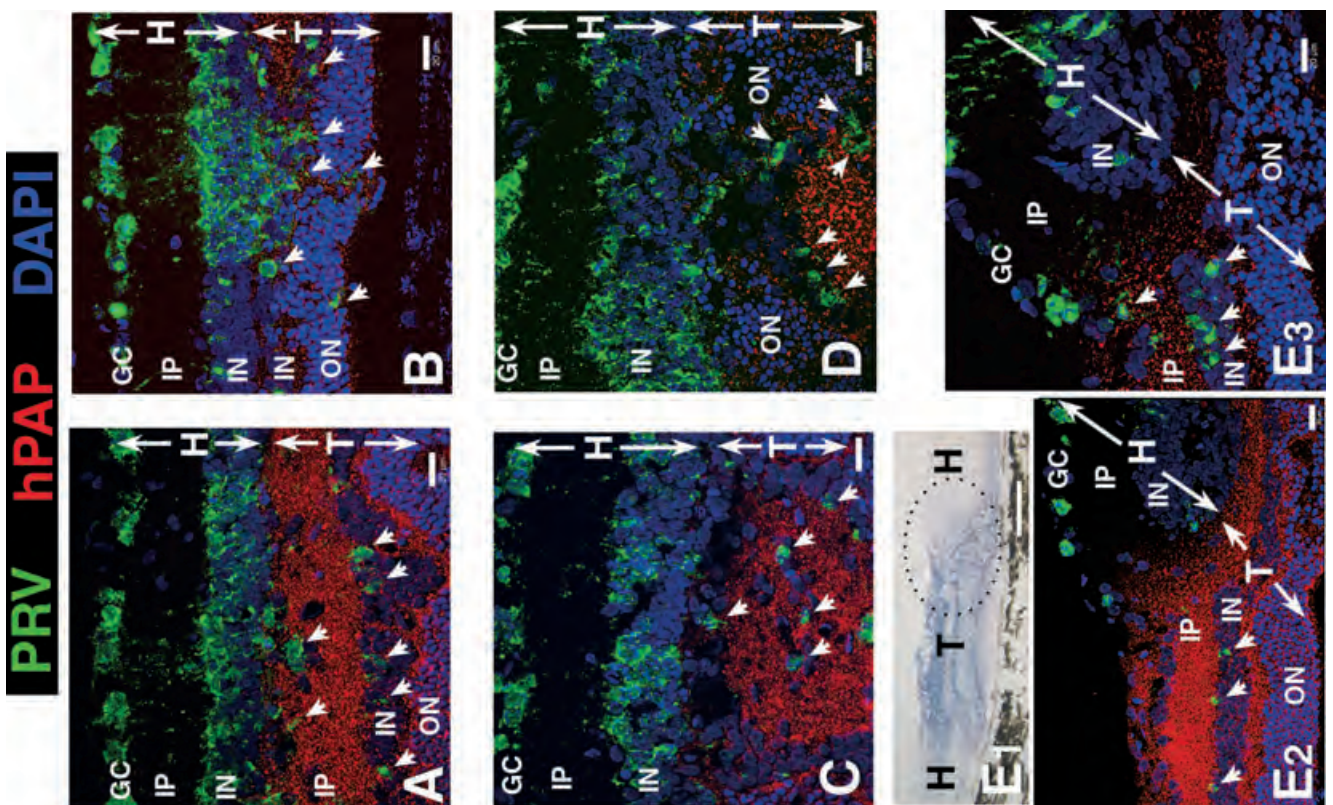
FIG. 6.



FIG. 5.

## Results

### Visual responses in the SC

An overview of the results is shown in Table 1. With the exception of rat no. 3 that had a threshold of $-1.1$ log cd/m$^2$, response thresholds ranged between $-1.7$ and $-3.5$ log cd/m$^2$ (mean $-3.1$ log cd/m$^2$) in a localized area of the SC (see Fig. 1). The penetration site with the lowest response threshold was selected for virus injection. Usually, the lowest threshold could only be found at one to four penetration sites, about 200 μm apart (see Fig. 1). Examples of visual responses at different light intensities are shown in Fig. 2.

The responses recorded from the SC of transplanted rats (from an area corresponding to the transplant location in the eye) were primarily of two distinct types, responses with robust spike activity (good responses) and responses with weak spike activity (weak responses) (see examples in Fig. 2). 'Good-response' recordings were characterized by robust spike activity in response to an increase in stimulus strength, whereas such an increase in spike activity was less apparent for 'weak responses' (Fig. 2). Most of the rats with good responses (three of four) also showed the lowest visual threshold of $-3.5$ log cd/m$^2$ (see Table 1), whereas the visual thresholds of weak-responding rats varied between $-1.1$ and 3.5 log cd/m$^2$.

### Virus label

The virus was injected into the location of the SC observed to have the lowest visual threshold (see above). The optimal survival time of 2 days after injection for the analysis of virus tracing was determined in previous experiments (Seiler et al., 2005). In all of the rats that were killed between 46 and 53 h after virus injection (12/14), the main virus label was confined to an area of the host retina overlying or adjacent to the transplant (examples in Fig. 3A and C). In all but two rats, virus-labeled cells were also found in the transplants (see Table 1), albeit with a lower label intensity than in the host retina.

Two rats had to be killed at an earlier time point (at 30 and 34 h after virus injection). In rat no. 1 (killed 30 h after virus injection), no virus-labeled cells were found in the transplant and only a few labeled host ganglion cells were found over the graft edge and in the proximity of the graft (Fig. 3E). Rat no. 2, killed 34 h after injection, showed clear label in the host ganglion cells and Muller cells overlying the transplant and one to two cells in the transplant (Fig. 3F). In the host retina adjacent to the transplant, some stained ganglion cells were observed (Fig. 3G); however, the labeling intensity was much less than over the transplant area, indicating a secondary neuronal infection from horizontal viral spread.

In the experiments with survival time of 2 days, there was a clear correlation between PRV label in the host and PRV label in the transplant ($r = 0.91$) but not between survival time and PRV label in the host ($r = 0.44$). There was no direct correlation between visual threshold and virus label in the host retina over ($r = -0.29$) or in ($r = -0.25$) the graft.

Based on the virus label in the graft with survival time of 2 days, rats were divided into two groups: poor/no labeling (0.5–8.7 PRV-positive cells in host ganglion cell layer (GCL)/section; 0–1.7 PRV-positive cells in graft/section) vs. moderate/good labeling (24.55–140.5 PRV-positive cells in host GCL/section; 3.2–55.3 cells PRV-positive cells in graft labeled/graft section) (see Table 1). A significantly lower visual threshold was observed in the SC of rats that had a stronger virus label in the host and transplant (see Fig. 4). However, this can only be a rough estimate because of differences between the experiments (survival time and virus label in the host retina).

### Double staining for PRV and various markers

The presence of virus-labeled cells in the transplant area was confirmed by double staining for PRV and hPAP (Fig. 5). In general, most virus-labeled cells in the transplant were found in the inner layers of the transplant and not in the photoreceptors. The hPAP label was seen as a diffuse cytoplasmic label, whereas the PRV label was mostly concentrated in the nucleus of cells.

Table 3 gives a semi-quantitative overview of PRV-immunoreactive cells in the transplants that double stained for the markers glutamine synthetase, calcium-calmodulin-dependent protein kinase II, protein kinase C, recoverin, microtubule-associated protein 2, parvalbumin, or marker for neuronal nuclei (NeuN). Double staining with the glial marker glutamine synthetase illustrated qualitatively that most of the virus-labeled cells in the transplants were not glial cells (Fig. 6), suggesting that they were probably neurons. On average, only 13% of the PRV-labeled cells also stained for glutamine synthetase (Table 3). Some of the PRV label was co-localized with protein kinase C (8.4%), a marker for rod bipolar cells (Fig. 7). Other PRV-labeled transplant cells were double stained for calcium-calmodulin-dependent protein kinase II (13.1%), a marker for ganglion and amacrine cells (Fig. 8). Relatively many transplant cells were double labeled for PRV and the neuronal markers microtubule-associated protein 2 (23.5%) and NeuN (25.1%), whereas very few were double stained for parvalbumin, a marker for A-II amacrine cells (0.9%) (see Table 3). No cells double labeled with calbindin (marker for horizontal and some amacrine cells) were found in the transplants (data not shown).

Almost no double staining in the transplant (3.3%) was observed with recoverin, a marker for cone bipolar and photoreceptor cells, although the transplant contained many recoverin-positive cells (Fig. 9A–D). However, recoverin-positive cone photoreceptors in the host retina were often heavily labeled (examples in Fig. 9A and C). In the host retina adjacent to the transplant, some PRV-labeled cells could be observed, mainly in the ganglion cell layer. PRV sometimes co-localized with cone bipolar cells (Fig. 9E).

---

FIG. 5. hPAP (donor cell label) (red) and PRV (green). White arrowheads indicate PRV-labeled cells in transplant. (A and B) Laminated transplants. (A) Rat no. 14 (same transplant as in Fig. 3C), labeled cells in transplant GCL and inner nuclear layer (IN). (B) Rat no. 10, labeled cells in transplant IN and outer nuclear layer (ON). Transplant ON close to host IN. (C and D) Rosetted transplants. (C) Rat no. 14 (same transplant as in Fig. 3C). (D) Rat no. 13. (E) 'Bridging' transplant (exposed to vitreous) of rat no. 10. (E1) hPAP histochemistry overview. (E2 and E3) Two different transplant areas. DAPI, 4′6-diamidino-2-phenylindole dihydrochloride; GC, ganglion cell layer; H, host; IN, inner nuclear layer; IP, inner plexiform layer; ON, outer nuclear layer; T, transplant. Bars, 20 μm.

---

FIG. 6. Glutamine synthetase (red) and PRV (green). Glutamine synthetase is a marker for glial cells. White arrowheads, double-stained cells in graft; black-on-white arrowheads, PRV-labeled cells in graft. (A) Rat no. 14, montage of laminated area (compare with Figs 5A and 3F). (B) Rat no. 10, laminated area (compare with Fig. 5B). (C) Rat no. 12 (not shown in Fig. 5). (D) Rat no. 14, rosetted area (compare with Fig. 5D). (E) Rat no. 10, bridging area (compare with Fig. 5E). DAPI, 4′6-diamidino-2-phenylindole dihydrochloride; GC, ganglion cell layer; Glusynth, glutamine synthetase; H, host; IN, inner nuclear layer; IP, inner plexiform layer; ON, outer nuclear layer; T, transplant. Bars, 20 μm.
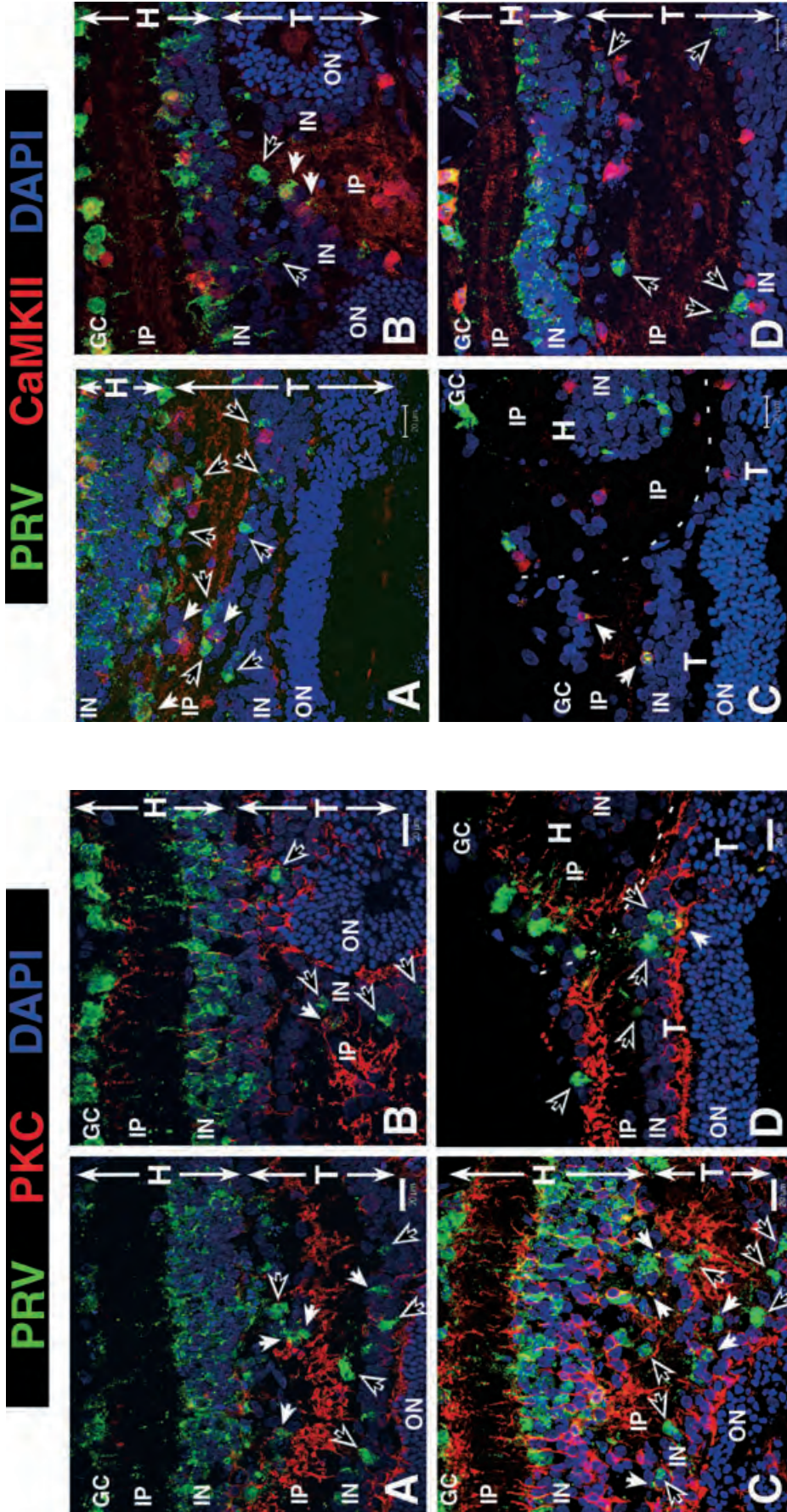
---

FIG. 8. Calcium-calmodulin-dependent protein kinase II (CaMKII) (a marker for ganglion and amacrine cells) (red) and PRV (green). White arrowheads, double-stained cells in graft; black-on-white arrowheads, PRV-labeled cells in graft. (A and B) Rat no. 14, laminated and rosetted area (two to three double-stained cells on each image). (C) Rat no. 10, bridge area (two double-stained cells). (D) Rat no. 12, rosetted area (no double-stained cells in graft). DAPI, 4'6-diamidino-2-phenylindole dihydrochloride; GC, ganglion cell layer; H, host; IN, inner nuclear layer; IP, inner plexiform layer; ON, outer nuclear layer; T, transplant. Bars, 20 μm.



FIG. 7. Protein kinase C (PKC) (red) and PRV (green). PKC is a marker for rod bipolar cells. White arrowheads, double-stained cells in graft; black-on-white arrowheads, PRV-labeled cells in graft. (A and B) Rat no. 14, laminated and rosetted area. (C) Rat no. 13, rosetted area. (D) Rat no. 10, bridge area. DAPI, 4'6-diamidino-2-phenylindole dihydrochloride; GC, ganglion cell layer; H, host; IN, inner nuclear layer; IP, inner plexiform layer; ON, outer nuclear layer; T, transplant. Bars, 20 μm.
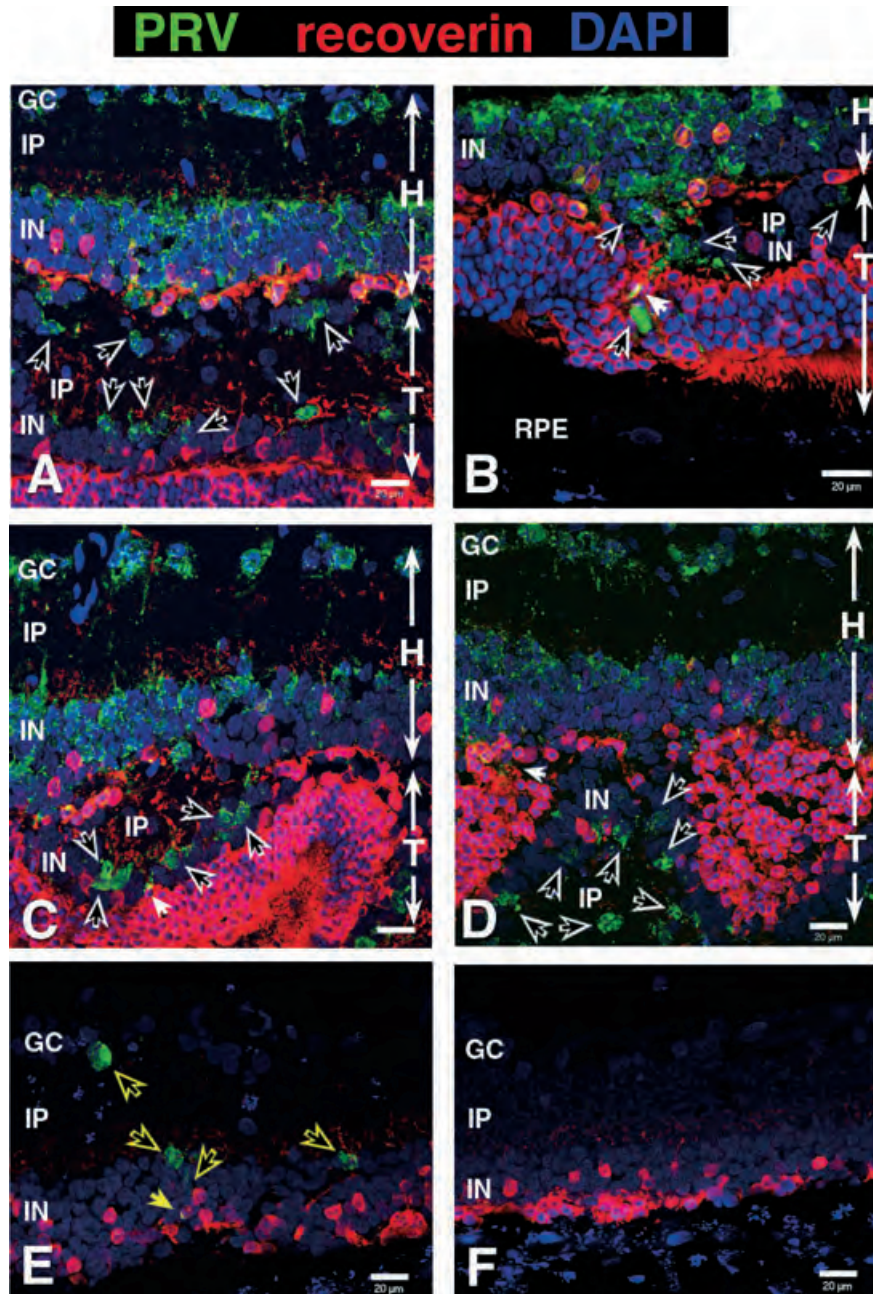
FIG. 9. Recoverin (red) (marker for photoreceptors and cone bipolar cells) and PRV (green) White arrowheads, double-stained cells in graft; black-on-white arrowheads, PRV-labeled cells in graft. Almost no double-stained cells in graft and clear double label of host cones. (A) Rat no. 14, laminated area. (B) Rat no. 10, laminated area. (C) Rat no. 14, rosetted area. (D) Rat no. 13, rosetted area. (E) Host retina close to graft (rat no. 13), few labeled cells. (F) Host retina far away from graft (no PRV label). DAPI, 4′6-diamidino-2-phenylindole dihydrochloride; GC, ganglion cell layer; H, host; IN, inner nuclear layer; IP, inner plexiform layer; ON, outer nuclear layer; RPE, retinal pigment epithelium; T, transplant. Bars, 20 μm.

## Discussion

This study demonstrates that the origin of SC visual responses to dim light stimulation in rats with retinal sheet transplants can be traced back to cells in the transplant in the subretinal space.

### Restoration of visual responses in the SC

Previous studies that demonstrated restoration of visual responses in the SC in transplanted rodents in different retinal degeneration models

(Woch *et al.*, 2001; Sagdullaev *et al.*, 2003; Arai *et al.*, 2004; Thomas *et al.*, 2004) used high-intensity light flashes (+ 3.1 log cd/m$^2$) that preferentially stimulate cones. As there are still cones left in the remaining host retina, it was not possible to exclude definitively that the transplant may have had its effect by rescuing host cones. In fact, rescue of host cones by sheet transplants has been shown in the *rd* mouse model (Arai *et al.*, 2004). However, in the three rat models of retinal degeneration (RCS, S334ter-line-3 and S334ter-line 5), no indication of cone rescue could be found by immunohistochemistry for S-antigen (rod arrestin), a marker for rods and cones (Woch *et al.*,

2001; Sagdullaev *et al.*, 2003; Thomas *et al.*, 2004). Furthermore, S334ter-line-3 retinas with BDNF-treated retinal progenitor sheets, which showed better functional outcomes (compared with grafts without BDNF treatment), also showed fewer red/green cones in the host retina over the transplant than outside the graft. The visual responses in the SC in these animals with BDNF-treated grafts corresponded topographically to the position of the transplant in the host retina, suggesting that the transplant effect was not due to the rescue of host cones (Seiler *et al.*, 2008). In addition, the above findings indicate that the cones present in the degenerate host retina (most of which are found outside the transplant) may not have any considerable visual functional capabilities. In summary, although we could not perform a systematic counting of cones in the current study, it is unlikely that transplant-specific visual responses were due to rescued cones in the light of the previous results.

As the transplants contain many rods (Seiler & Aramant, 1998; Seiler *et al.*, 1999; Sagdullaev *et al.*, 2003) and the host retina has lost all of its rods by the time of transplantation (Sagdullaev *et al.*, 2003), testing using dim light (scotopic) intensities may allow selective assessment of the direct effect of transplanted photoreceptors. Thus, in this study, we tested dark-adapted transplanted rats for their visual threshold and responses to lower-intensity light stimulation.

The S334ter-line-3 transplant recipients have a threshold of $-1$ log cd/m$^2$ at the age of 4 weeks when the transplantation is performed (unpublished data) and have still weaker responses at the higher threshold of 0 log cd/m$^2$ by the age of 11 weeks (Thomas *et al.*, 2006). In the current study, the age of the transplanted rats at the time of recording ranged between 12 and 23 weeks, and the visual thresholds found only in a small area of the SC corresponding to the graft location ranged between $-1.1$ and $-3.5$ log cd/m$^2$, with an average of $-3.1$. This suggests that the transplants have increased the visual sensitivity to light in a specific area of the SC that had been much less sensitive at the time of transplantation. This response threshold corresponds to a mesopic light level that stimulates both rods and cones.

Other groups have also reported restoration of visual responses by transplants but with different testing methods (Silverman *et al.*, 1992; Kwan *et al.*, 1999; Radner *et al.*, 2001; MacLaren *et al.*, 2006). For example, MacLaren *et al.* (2006) cited increased host retinal ganglion cell responses and pupillary reflexes following the injection of freshly harvested retinal progenitor cells in the rho$-/-$ mouse as evidence of visual improvement. The reliability of retinal ganglion cell recordings and pupillary responses as measures of visual recovery, however, has been questioned by other investigators (Kovalevsky *et al.*, 1995; An *et al.*, 2002; Gaillard & Sauve, 2007).

### Trans-synaptic PRV tracing from visually responsive site

This study builds on findings from a previous study that demonstrated the existence of apparent synaptic connections between transplant and host by PRV tracing from the SC (Seiler *et al.*, 2005). In the previous study, the virus was injected into an area of the SC that was estimated to correspond topographically to the transplant area in the retina. This was not confirmed, however, by electrophysiological testing. As a result, the transplant area in the host retina was missed in 13 of 33 experiments. In contrast, in all experiments of the current study, the main virus label of the host retina was found over the transplant because the optimal recording site had been identified in the SC by electrophysiological recording before the virus injection.

The focal point of the virus label, however, was not always found precisely over the center of the transplant, which was possibly due to several reasons: (i) because of biosafety concerns, the rat had to be transferred to a different room into a different stereotaxic apparatus

and the site of the lowest threshold was determined based on blood vessel landmarks on the surface of the SC that were sometimes difficult to redetermine exactly; (ii) a possible difference in the depth or angle of the injection needle may influence the target location in the retina and (iii) the lumen of the injection capillary was much larger (70 μm) than the tip size of the recording electrode (< 1.0 μm).

The trans-synaptic spread of the virus after injection occurred in both the retina and SC (see also Seiler *et al.*, 2005), i.e., with time, the virus spread to neurons in other areas of the SC that then labeled their connected ganglion cells later. This explains the observation of labeling of additional ganglion cells beyond the primary virus label site in the host retina.

In many cases, the virus label spread to host cones overlying the transplant as well as to transplant neurons, suggesting that the host cones might also contribute to visual responses (see examples in Fig. 9A). However, there were also cases where few host cones were labeled or there were more labeled cells in the transplant compared with the host (Fig. 9C and D).

### Intensity of virus label in the transplant

As previous publications have established (Card, 1998; Chen *et al.*, 1999), the time after virus injection (together with the initial virus concentration) determines the intensity of label in the host retina. The replication cycle of PRV in a neuron is approximately 6 h (Aston-Jones & Card, 2000), with PRV antigen appearing first in the nucleus, then the cytoplasm and lastly in the dendritic tree (Aston-Jones & Card, 2000). However, there were several experiments with poor label of the host retina after the optimal survival time of 2 days. Some virus could possibly have seeped out of the tissue when the tip of the glass injection needle was withdrawn, despite our precaution of waiting for 5 min before removing the injection needle. If that were the case, the titer of virus in the colliculus would be substantially diluted, which would probably be reflected in a reduction in either the onset or magnitude of viral replication and transport.

If the virus titer is reduced, it directly affects the virus transfer (Card *et al.*, 1995, 1999). The three experiments with no virus label in the transplant also had poor virus label of the host retina. Three additional experiments had few virus-labeled cells. In two of these, the center of virus label was in the host retina over the transplant but relatively minimal virus label had reached the host retina. In the third experiment, the main label was found at the edge of the transplant.

A significantly lower visual threshold (i.e., higher light sensitivity) was observed in the SC of rats that had more intense virus label in the transplant (Fig. 4). Most of the rats in this group also had a stronger label of the host retina.

### Double staining of cells for hPAP donor label and PRV

The PRV-stained nuclei were found completely surrounded by hPAP-stained cytoplasm and were interpreted as PRV-labeled transplant cells for the following reasons. The hPAP label of the donor tissue is a cytoplasmic label, whereas the PRV label was mainly found in the nuclei. The argument can be made that, because there is intense remodeling in the host retina (Jones & Marc, 2005), host cells may migrate into the transplant and thus be labeled by PRV. If the PRV-labeled cells had migrated from the host retina, they would still have kept their synaptic connections with host cells. The intensity of staining and their staining sequence should have corresponded to the host inner nuclear layer. This was not the case, arguing against the possibility of host cells migrating into the transplant.

## Specificity of virus label for indicating synaptic connectivity

The specific properties of PRV prevent non-specific diffusion from the injection site (Aston-Jones & Card, 2000). Virus spread only occurs through synaptic transfer. Although glial cell processes can pick up virus in the perisynaptic space, they lack the machinery to produce infectious virus to exit the cell and thus prevent non-synaptic spread (Card *et al.*, 1993). Virus transfer can only occur along mature synapses and close proximity of cell processes is not sufficient (Rinaman *et al.*, 2000).

As PRV can be transferred to glial cells enclosing a synapse, it was important to verify the identity of virus-labeled cells in the transplants by double labeling with glial and neuronal markers.

## Labeled cell types and possible circuitry for restored visual responses

It was beyond the scope of this study to perform a thorough quantitative analysis but our experimental data indicate that the majority of virus-labeled cells in the transplants were non-glial, i.e., neurons, because only 13.25% of PRV-immunoreactive cells in the transplants were double stained for glutamine synthetase. Double labeling for diverse bipolar and amacrine cell markers was observed. However, almost no transplant photoreceptors were double labeled. This indicates that transplant photoreceptors do not connect with host interneurons directly but that there are probably connections between transplant interneurons and host interneurons, e.g., bipolar cells, through which the visual signals from the transplanted photoreceptors may be transmitted. Previous studies indicate that very few, if any, retinal ganglion cells survive in the transplants (unpublished data). It is therefore important that the transplanted retinal progenitor sheet transplants develop both photoreceptors and retinal interneurons. However, the ramifications of transplant-interneuron-to-host-interneuron signaling on the quality of the visual information transmitted is still unknown.

In future studies, more detailed analysis will be required at the electron microscopic level to identify cell types involved in synaptic connections between transplant and host, using a combination of donor tissue (hPAP) and various cellular and synaptic markers.

In summary, this study has confirmed that the origin of SC visual responses in transplanted retinal-degenerate rats can be traced back to transplant cells. The findings indicate that synaptic connectivity between the transplant and host contributes to the visual responses.

## Acknowledgements

## Abbreviations

BDNF, brain derived neurotrophic factor; GC or GCL, ganglion cell layer; GFP, green fluorescent protein; hPAP, human placental alkaline phosphatase; IN, inner nuclear layer; IP, inner plexiform layer; ON, outer nuclear layer; PRV, pseudorabies virus; RPE, retinal pigment epithelium; SC, superior colliculus.

## References

An, G.J., Asayama, N., Humayun, M.S., Weiland, J., Cao, J., Kim, S.Y., Grebe, R., de Juan, E. Jr. & Sadda, S. (2002) Ganglion cell responses to retinal light stimulation in the absence of photoreceptor outer segments from retinal degenerate rodents. *Curr. Eye Res.*, **24**, 26–32.

Arai, S., Thomas, B.B., Seiler, M.J., Aramant, R.B., Qiu, G., Mui, C., de Juan, E. & Sadda, S.R. (2004) Restoration of visual responses following transplantation of intact retinal sheets in rd mice. *Exp. Eye Res.*, **79**, 331–341.

Aramant, R.B. & Seiler, M.J. (1995) Fiber and synaptic connections between embryonic retinal transplants and host retina. *Exp. Neurol.*, **133**, 244–255.

Aramant, R.B. & Seiler, M.J. (2002) Retinal transplantation – advantages of intact fetal sheets. *Prog. Retin. Eye Res.*, **20**, 57–73.

Aramant, R.B. & Seiler, M.J. (2004) Progress in retinal sheet transplantation. *Prog. Retin. Eye Res.*, **23**, 475–494.

Aramant, R.B., Seiler, M.J. & Ball, S.L. (1999) Successful cotransplantation of intact sheets of fetal retinal pigment epithelium with retina. *Invest. Ophthalmol. Vis. Sci.*, **40**, 1557–1564.

Aramant, R.B., Radtke, N.D. & Seiler, M.J. (2006) Recent results in retinal transplantation give hope for restoring vision. In Tombran-Tink, J. & Barnstable, C.J. (Eds), *Retinal Degenerations: Genetics, Progression, and Therapeutics*. Humana Press, Totowa, NJ, pp. 363–381.

Aston-Jones, G. & Card, J.P. (2000) Use of pseudorabies virus to delineate multisynaptic circuits in brain: opportunities and limitations. *J. Neurosci. Methods*, **103**, 51–61.

Cano, G., Card, J.P. & Sved, A.F. (2004) Dual viral transneuronal tracing of central autonomic circuits involved in the innervation of the two kidneys in rat. *J. Comp. Neurol.*, **471**, 462–481.

Card, J.P. (1998) Practical considerations for the use of pseudorabies virus in transneuronal studies of neural circuitry. *Neurosci. Biobehav. Rev.*, **22**, 685–694.

Card, J.P. & Enquist, L.W. (1994) Use of pseudorabies virus for definition of synaptically linked populations of neurons. In Adolph, K.W. (ed.) *Methods in Molecular Genetics*. Academic Press, New York, NY, pp. 363–382.

Card, J.P., Rinaman, L., Schwaber, J.S., Miselis, R.R., Whealy, M.E., Robbins, A.K. & Enquist, L.W. (1990) Neurotropic properties of pseudorabies virus: uptake and transneuronal passage in the rat central nervous system. *J. Neurosci.*, **10**, 1974–1994.

Card, J.P., Rinaman, L., Lynn, R.B., Lee, B.H., Meade, R.P., Miselis, R.R. & Enquist, L.W. (1993) Pseudorabies virus infection of the rat central nervous system: ultrastructural characterization of viral replication, transport, and pathogenesis. *J. Neurosci.*, **13**, 2515–2539.

Card, J.P., Dubin, J.R., Whealy, M.E. & Enquist, L.W. (1995) Influence of infectious dose upon productive replication and transynaptic passage of pseudorabies virus in rat central nervous system (see comments). *J. Neurovirol.*, **1**, 349–358.

Card, J.P., Enquist, L.W. & Moore, R.Y. (1999) Neuroinvasiveness of pseudorabies virus injected intracerebrally is dependent on viral concentration and terminal field density. *J. Comp. Neurol.*, **407**, 438–452.

Chen, S., Yang, M., Miselis, R.R. & Aston-Jones, G. (1999) Characterization of transsynaptic tracing with central application of pseudorabies virus. *Brain Res.*, **838**, 171–183.

Gaillard, F. & Sauve, Y. (2007) Cell-based therapy for retina degeneration: the promise of a cure. *Vision Res.*, **47**, 2815–2824.

Ghosh, F., Bruun, A. & Ehinger, B. (1999) Graft-host connections in long-term full-thickness embryonic rabbit retinal transplants. *Invest. Ophthalmol. Vis. Sci.*, **40**, 126–132.

Ghosh, F., Wong, F., Johansson, K., Bruun, A. & Petters, R.M. (2004) Transplantation of full-thickness retina in the rhodopsin transgenic pig. *Retina*, **24**, 98–109.

Gouras, P. & Tanabe, T. (2003) Survival and integration of neural retinal transplants in rd mice. *Graefes Arch. Clin. Exp. Ophthalmol.*, **241**, 403–409.

Hakamata, Y., Tahara, K., Uchida, H., Sakuma, Y., Nakamura, M., Kume, A., Murakami, T., Takahashi, M., Takahashi, R., Hirabayashi, M., Ueda, M., Miyoshi, I., Kasai, N. & Kobayashi, E. (2001) Green fluorescent protein-transgenic rat: a tool for organ transplantation research. *Biochem. Biophys. Res. Commun.*, **286**, 779–785.

Humayun, M.S., Prince, M., de Juan, E. Jr., Barron, Y., Moskowitz, M., Klock, I.B. & Milam, A.H. (1999) Morphometric analysis of the extramacular retina from postmortem eyes with retinitis pigmentosa. *Invest. Ophthalmol. Vis. Sci.*, **40**, 143–148.

Jones, B.W. & Marc, R.E. (2005) Retinal remodeling during retinal degeneration. *Exp. Eye Res.*, **81**, 123–137.

Kim, J.S., Enquist, L.W. & Card, J.P. (1999) Circuit-specific coinfection of neurons in the rat central nervous system with two pseudorabies virus recombinants. *J. Virol.*, **73**, 9521–9531.

Kisseberth, W.C., Brettingen, N.T., Lohse, J.K. & Sandgren, E.P. (1999) Ubiquitous expression of marker transgenes in mice and rats. *Dev. Biol.*, **214**, 128–138.

Klassen, H.J., Ng, T.F., Kurimoto, Y., Kirov, I., Shatos, M., Coffey, P. & Young, M.J. (2004) Multipotent retinal progenitors express developmental markers, differentiate into retinal neurons, and preserve light-mediated behavior. *Invest. Ophthalmol. Vis. Sci.*, **45**, 4167–4173.

Kovalevsky, G., DiLoreto, D. Jr., Wyatt, J., del Cerro, C., Cox, C. & del Cerro, M. (1995) The intensity of the pupillary light reflex does not correlate with the number of retinal photoreceptor cells. *Exp. Neurol.*, **133**, 43–49.

Kwan, A.S., Wang, S. & Lund, R.D. (1999) Photoreceptor layer reconstruction in a rodent model of retinal degeneration. *Exp. Neurol.*, **159**, 21–33.

Loewy, A.D., Bridgman, P.C. & Mettenleiter, T.C. (1991) beta-Galactosidase expressing recombinant pseudorabies virus for light and electron microscopic study of transneuronally labeled CNS neurons. *Brain Res.*, **555**, 346–352.

MacLaren, R.E., Pearson, R.A., MacNeil, A., Douglas, R.H., Salt, T.E., Akimoto, M., Swaroop, A., Sowden, J.C. & Ali, R.R. (2006) Retinal repair by transplantation of photoreceptor precursors. *Nature*, **444**, 203–207.

Mahoney, M.J. & Saltzman, W.M. (2001) Transplantation of brain cells assembled around a programmable synthetic microenvironment. *Nat. Biotechnol.*, **19**, 934–939.

Marchand, C.F. & Schwab, M.E. (1986) Binding, uptake and retrograde axonal transport of herpes virus suis in sympathetic neurons. *Brain Res.*, **383**, 262–270.

McGinnis, J.F., Stepanik, P.L., Jariangprasert, S. & Lerious, V. (1997) Functional significance of recoverin localization in multiple retina cell types. *J. Neurosci. Res.*, **50**, 487–495.

Milam, A.H., Li, Z.Y. & Fariss, R.N. (1998) Histopathology of the human retina in retinitis pigmentosa. *Prog. Retin. Eye Res.*, **17**, 175–205.

O'Leary, D.D., Fawcett, J.W. & Cowan, W.M. (1986) Topographic targeting errors in the retinocollicular projection and their elimination by selective ganglion cell death. *J. Neurosci.*, **6**, 3692–3705.

Pickard, G.E., Smeraski, C.A., Tomlinson, C.C., Banfield, B.W., Kaufman, J., Wilcox, C.L., Enquist, L.W. & Sollars, P.J. (2002) Intravitreal injection of the attenuated pseudorabies virus PRV Bartha results in infection of the hamster suprachiasmatic nucleus only by retrograde transsynaptic transport via autonomic circuits. *J. Neurosci.*, **22**, 2701–2710.

Radner, W., Sadda, S.R., Humayun, M.S., Suzuki, S., Melia, M., Weiland, J. & de Juan, E. Jr. (2001) Light-driven retinal ganglion cell responses in blind rd mice after neural retinal transplantation. *Invest. Ophthalmol. Vis. Sci.*, **42**, 1057–1065.

Rinaman, L., Levitt, P. & Card, J.P. (2000) Progressive postnatal assembly of limbic-autonomic circuits revealed by central transneuronal transport of pseudorabies virus. *J. Neurosci.*, **20**, 2731–2741.

Sagdullaev, B.T., Aramant, R.B., Seiler, M.J., Woch, G. & McCall, M.A. (2003) Retinal transplantation induces recovery of retino-tectal visual function in a rodent model of retinitis pigmentosa. *Invest. Ophthalmol. Vis. Sci.*, **44**, 1686–1695.

Seiler, M.J. & Aramant, R.B. (1998) Intact sheets of fetal retina transplanted to restore damaged rat retinas. *Invest. Ophthalmol. Vis. Sci.*, **39**, 2121–2131.

Seiler, M.J. & Aramant, R.B. (2005) Transplantation of neuroblastic progenitor cells as a sheet preserves and restores retinal function. *Semin. Ophthalmol.*, **20**, 31–42.

Seiler, M.J., Aramant, R.B. & Ball, S.L. (1999) Photoreceptor function of retinal transplants implicated by light-dark shift of S-antigen and rod transducin. *Vision Res.*, **39**, 2589–2596.

Seiler, M.J., Sagdullaev, B.T., Woch, G., Thomas, B.B. & Aramant, R.B. (2005) Transsynaptic virus tracing from host brain to subretinal transplants. *Eur. J. Neurosci.*, **21**, 161–172.

Seiler, M.J., Thomas, B.B., Chen, Z., Arai, S., Chadalavada, S., Mahoney, M.J., Sadda, S.R. & Aramant, R.B. (2008) BDNF-treated retinal progenitor sheets transplanted to degenerate rats – improved restoration of visual function. *Exp. Eye Res.*, **86**, 92–104.

Shu, X.Z., Liu, Y., Luo, Y., Roberts, M.C. & Prestwich, G.D. (2002) Disulfide cross-linked hyaluronan hydrogels. *Biomacromolecules*, **3**, 1304–1311.

Silverman, M.S., Hughes, S.E., Valentino, T. & Liu, Y. (1992) Photoreceptor transplantation: anatomic, electrophysiologic, and behavioral evidence for the functional reconstruction of retinas lacking photoreceptors. *Exp. Neurol.*, **115**, 87–94.

Simon, D.K. & O'Leary, D.D. (1992) Development of topographic order in the mammalian retinocollicular projection. *J. Neurosci.*, **12**, 1212–1232.

Thomas, B.B., Seiler, M.J., Sadda, S.R. & Aramant, R.B. (2004) Superior colliculus responses to light – preserved by transplantation in a slow degeneration rat model. *Exp. Eye Res.*, **79**, 29–39.

Thomas, B.B., Aramant, R.B., Sadda, S.R. & Seiler, M.J. (2005) Light response differences in the superior colliculus of albino and pigmented rats. *Neurosci. Lett.*, **385**, 143–147.

Thomas, B.B., Aramant, R.B., Sadda, S.R. & Seiler, M.J. 2006. Retinal transplantation – a treatment strategy for retinal degenerative diseases. In Hollyfield, J.G., Anderson, R.E. & LaVail, M.M. (Eds), *Retinal Degenerative Diseases*. Springer, New York, NY, pp. 367–376.

Viney, T.J., Balint, K., Hillier, D., Siegert, S., Boldogkoi, Z., Enquist, L.W., Meister, M., Cepko, C.L. & Roska, B. (2007) Local retinal circuits of melanopsin-containing ganglion cells identified by transsynaptic viral tracing. *Curr. Biol.*, **17**, 981–988.

Woch, G., Aramant, R., Seiler, M., Sagdullaev, B. & McCall, M. (2001) Retinal transplants restore visually evoked responses in rats with photoreceptor degeneration. *Invest. Ophthalmol. Vis. Sci.*, **42**, 1669–1676.